Journal of Thermal Analysis and Calorimetry, Vol. 81 (2005) 75–82

ENERGETICS OF MODEL COMPOUNDS OF WATER OXIDIZING COMPLEX CONTAINING QUINONE COFACTORS TG-DTA and PXRD studies

A. V. Todkary[1], *S. B. Zaware*[1], *D. R. Thube*[1,2], *J. V. Yakhmi*[3] *and S. Y. Rane*[1*]

[1]Department of Chemistry, University of Pune, Pune 411 007, India
[2]Department of Chemistry, New Arts, Com. and Science College, Parner, Ahmednagar 414302, India.
[3]Technical Physics and Prototype Engg. Division, Bhaha Atomic Research Centre, Trombay, Mumbai 400085, India

To reveal reaction mechanism of PS-II, the reaction products of photolysis may be compared with their thermolytic products. According to required molecular assemblies in manganese clusters at WOC of PS-II, we have strategically synthesized dimers (**M-1**, **M-2**), trimers (**M-3A**, **M-3B**) and tetramer (**M-4**) using spin carrier imino-phenol functionalized ligands viz. Lawsone Oxime (L-1) and Phthiocol Oxime (L-2) of naturally occurring quinones .These are characterized by elemental analyses, thermogravimetric analyses, differential thermal analyses, powder X-ray diffraction and infrared spectroscopy. Stabilization energies for molecular associations of ligands in various redox and stereoisomeric forms via hydrogen bondings are compared with thermal energies required for their expulsion from the coordination polymers calculated with the help of Coats and Redfern's relation of rising temperatures. Activation energy required for establishing tetramer (**M-4**) and dimer (**M-2**) in coordination sphere by counter ion using same synthetic route is found to be comparable (~37.48±1 kJ mol^{-1}). Quantitized energies from TG-DTA data for valence tautomers of redox active ligands play significant role in formation of resultant model compound. viz. tetramer, dimer of dimer and trimer. The role of oxo, acetato and spin carrier ligands in model cluster compounds are proposed with respect to their expulsion energies.

Keywords: *activation energy (E_a), H-bonding, PS-II, redox forms of hydroxy naphthoquinone, WOC*

Introduction

Efforts to model the active site of the water oxidizing complex (WOC) have resulted in many interesting structural types for mixed valent clusters of manganese [1]. Such transition metal complexes have substantial covalent bond character [2]. This has important implications for oxidation – reduction catalysis by manganese proteins such as the OEC (oxygen evolving complex) [3] of photosystem –II (PS-II). The degree of covalency for manganese – oxygen bonds that is indicated from charge density consideration [4] precludes the presence of the electropositive centre of high- valent manganese in biological complexes. Recent reports [5] reveal that manganese ion in the OEC are bound to O and/or N donor atoms from the amino acid residues containing hydrogen bonded tyrosyl radical and spin carrier quinones, we have therefore, synthesized manganese complexes using quinone based ligands containing O^N donor atoms viz, Lawsone oxime (L-1) and phthiocol oxime (L-2). These organic cofactors become important as they may exist in fully oxidized *para*-naphthoquinone (NQ), one electron reduced naphthosemiquinone (NSQ) as well as fully reduced catecholate (CAT) forms [6–7] (cf. Scheme 1) and also perform the hydrogen bonding network that can lead to formation of supramolecular assemblies [8] as required for WOC compound. From the non-isothermal TG studies coupled with infrared studies of dimers **M-1**: $[Mn_2(OAc)_3(L\text{-}1)_2]$, **M-2**: $[(C_2H_5)_4N][Mn_2O_2(OAc)_2(L\text{-}2)_2]$, trimers **M-3A**: $[Mn_3(OAc)_6(L\text{-}1)_3]$, **M-3B**: $[Mn_3(OAc)_6(L\text{-}2)_3]$ and tetramer **M-4**: $[(C_2H_5)_4N][Mn_4O_2(OAc)_6(L\text{-}1)_2]$ of manganese we have investigated mimic of energetics in PS-II

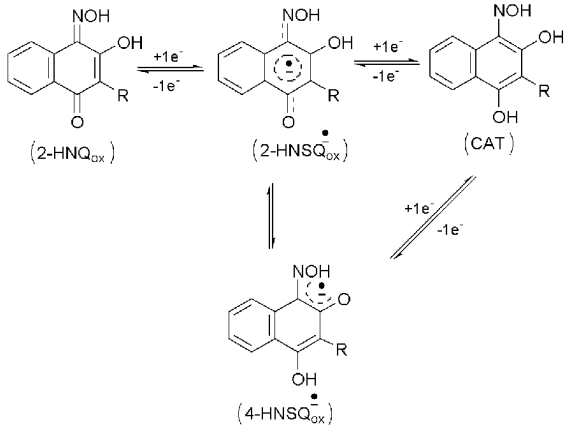

Scheme 1 Redox active forms of 2-hydroxy-4-naphthoquinone-1-oxime where *R*=CH_3=phthiocol and *R*=H=lawsone

* Author for correspondence: syrane@chem.unipune.ernet.in

1388–6150/$20.00

Akadémiai Kiadó, Budapest, Hungary
Springer, Dordrecht, The Netherlands

photochemistry that primarily uses O^O, O^N donor sets to the metal as possible models for the manganese centre in the OEC.

Experimental

Chemicals

All the chemicals used in the preparation of metal complexes are of analytical grade. 2-hydroxy-1,4-naphtho-quinone (Lawsone) and manganese (III) acetate dihydrate [$Mn(OAc)_3 \cdot 2H_2O$] were obtained commercially from sigma and used without further purification. Solvents were distilled and dried according to the literature [9]. L-1 and L-2 were prepared according to procedure reported earlier [10]. Tetra ethyl ammonium permanganate [$(C_2H_5)_4N \cdot MnO_4$] was prepared as outlined in the literature [11].

Analytical data

The chemical compositions of **M-1**, **M-2**, **M-3A**, **M-3B** and **M-4** were established from their elemental analyses (*cf*. Table 1). Carbon, hydrogen and nitrogen were determined using German model Elementar Vario EL analyzer. The manganese ratio was determined by atomic absorption spectroscopy (AAS) using a PerkinElmer 33100 apparatus after dissolution of the samples in aqua regia and conc. sulphuric acid in order to destroy the organic part.

Synthesis

M-1, $[Mn_2(OAc)_3(L\text{-}1)_2]$

To the ethanolic solution of L-1 (0.189 g, 1.0 mmol), solution of $Mn(OAc)_3 \cdot 2H_2O$ (0.268 g, 1 mmol) was added drop wise. The mixture was stirred for two hours under aerobic conditions. Dark brown solution thus obtained was evaporated under vacuum which yielded deep brown crystals. The product was then washed with cold water and ether.

M-2, $[(C_2H_5)_4N][Mn_2O_2(OAc)_2(L\text{-}2)_2]$

To a stirred equimolar solutions of sodium methoxide (0.108 g, 2 mmol) and L-2 (0.406 g, 2 mmol) in methanol (~50 mL), $Mn(OAc)_2 \cdot 4H_2O$ (0.784 g, 3.2 mmol), glacial acetic acid (1 mL, 17 mmol) and solid $[(C_2H_5)_4N]MnO_4$ (0.199 g, 0.8 mmol) were added simultaneously, solution turned deep brown. After one hour, solution of tetraethyl ammonium bromide (0.840 g, 4 mmol) in 10 mL of water was added. The reaction mixture was stirred in air for two hours and freezed for 36 h which yielded deep brown crystals which was washed with cold water and ether.

M-3A, $[Mn_3(OAc)_6(L\text{-}1)_3]$

To a solution of manganese (II) acetate tetrahydrate (0.0539 g, 0.22 mmol), methanolic solution of L-1 (0.189 g, 1 mmol) was added. This orange coloured mixture on addition of $[(C_2H_5)_4N]MnO_4$ (0.0274 g, 0.11 mmol) with constant stirring gave a black homogeneous solution which on stirring for few minutes results in formation of black microcrystalline precipitate, collected by filtration, washed with water and dried under vacuum for 45 min.

M-3, $[Mn_3(OAc)_6(L\text{-}2)_3]$

A procedure similar to **M-3A** was followed wherein, L-1 was replaced by L-2.

M-4, $[(C_2H_5)_4N][Mn_4O_2(OAc)_6(L\text{-}1)_2]$

A procedure similar to **M-2** was carried out using L-1 as a chelating ligand. The product obtained as black needles after freezing for 36 h was washed with cold water and ether.

Infrared spectra

The infrared spectrum of the ligands and their metal complexes were recorded as KBr pellet on an IR-470 Schimadzu infrared spectrophotometer.

Table 1 Yields in % on preparation, appearance and analytical data of **M-1**, **M-2**, **M-3A**, **M-3B** and **M-4** compounds

Compound[a]	Yield	Appearance[b]	C		H		N		Mn	
			calc.[c]	found	calc.[c]	found	calc.[c]	found	calc.[c]	found
M-1	80	dbr. crs.	47.07	47.00	3.19	2.90	4.22	4.08	16.56	15.80
M-2	60	br. crs.	51.30	51.42	5.32	5.23	5.28	5.93	13.82	14.40
M-3A	90	bl. pw.	46.58	46.04	3.07	3.97	3.88	4.19	15.21	13.71
M-3B	40	gre. crs.	48.04	48.63	3.90	3.64	3.73	4.27	14.65	14.44
M-4	70	bl. crs.	43.19	43.98	4.53	4.49	3.77	4.06	19.75	17.85

[a]**M-1**, $[Mn_2(OAc)_3(L\text{-}1)_2]$; **M-2**, $[(C_2H_5)_4N][Mn_2O_2(OAc)_2(L\text{-}2)_2]$; **M-3A**, $[Mn_3(OAc)_6(L\text{-}1)_3]$; **M-3B**, $[Mn_3(OAc)_6(L\text{-}2)_3]$; **M-4**, $[(C_2H_5)_4N][Mn_4O_2(OAc)_6(L\text{-}1)_2]$; [b]Key: bl. – black; dbr. – dark brown; br. – brown; gre. – green; crs. – crystals; pw. – powder, [c]calc. – calculated

Thermal studies

Thermal analysis was performed at two different heating rates on a) simultaneous TG-DTA-EGA thermal analyzer, Netzsch thermobalance, Model STA-409, Germany, under air atmosphere. (Temperature sensor: Pt *vs*. Pt 10% Rh) with the samples varying in mass from 10.2–22.5 mg and a heating rate: 10°C min^{-1} and b) a laboratory built thermo balance, with the heating rate of 3–5°C min^{-1} and 30–50 mg samples of 250–200 mesh particle size details of which have been reported [12, 13].

Powder X-ray diffraction studies

The powder X-ray diffraction (PXRD) pattern was registered by means of a PW 1840 diffractometer operated at 30 kV and 30 mA using a CuK_α radiation at a scanning speed of 2º(2θ) min^{-1}.

Results and discussion

The energetics in PS-II photochemistry is concerned with its water oxidation function, where water as substrate in WOC of manganese cluster requires binding energy of ~0.3 eV i.e. 28.94 kJ mol^{-1} [14]. Hydrogen bondings are significant in formation of supramolecular assemblies where weak interactions needed 10 to 50 kJ mol^{-1} energies which are comparable to thermal energies [15, 16]. The biological significance of the quinones in PS-II relates to their one (SQ) or two (CAT) electron- acceptor capabilities, which in turn, help in electron transport. Here, we are reporting the relevance of energetics of WOC model compounds from the pyrolytic reactions of manganese compounds (**M-1** to **M-4**) with photolytic reactions in PS-II.

Infrared spectra

The IR spectral criteria has been used for assignments of $NQ_{ox}/NSQ^{\cdot-}_{ox}$ type of coordination from our former report [17] which supports the TGA data and confirms $NSQ^{\cdot-}_{ox}$ coordination of L-1 and L-2 ligands in **M-1**, **M-3A**, **M-3B** and **M-4**, however, NQ_{ox} coordinations of L-2 ligand in **M-2**. The selected vibrational frequencies for all the complexes are displayed in Table 2. A broad band of medium intensity observed at 3125–3517 cm^{-1} arises due to free oximino hydroxyl group. Shift in the vibrational frequencies for ν(C–O) (at C-2 position) and $\nu_{(C=N)}$ (at C-1 position) suggest the formation of complexes (**M-1** to **M-4**) by coordination through oxygen (at C-2 position) and oximino nitrogen of L-1 and L-2 with the metal. A red shift is observed for $\nu_{(N–O)}$ vibration in **M-1**, **M-3A**, **M-3B** and **M-4**, where, ligand coordinates in naphthosemiquinone oxime ($NSQ^{\cdot-}_{ox}$) form which is in contrast with **M-2** where a blue shift indicates existence of L-2 in fully oxidized naphthoquinone oxime (NQ_{ox}) form. Lowering of intensity in former compounds as compared to that in the latter is noteworthy. A strong band at 615 and 623 cm^{-1} indicates presence of oxo-bridges in **M-2** and **M-4** complexes [18], however these bands are absent in **M-1**, **M-3A** and **M-3B**.

Thermal analysis

Non-isothermal TG studies

The simultaneous non–isothermal TG-DTA curves for the solid phase thermal decomposition of **M-1**, **M-2** and **M-4** and TG curves for **M-3A**, **M-3B** are displayed in Fig. 1. The dynamic TG data with per-

Table 2 Selected infrared frequencies (in cm^{-1}) in L-1, L-2, **M-1**, **M-2**, **M-3A**, **M-3B** and **M-4**

	L-1	L-2	**M-1**	**M-2**	**M-3A**	**M-3B**	**M-4**
ν_s OH $_{(inter)}$	3517 (w)	3365 (m)				3336 (mbr)	3409 (mbr)
$_{(intra)}$	3143 (mbr)	3125 (sbr)	3219 (wbr)	3298 (wbr)	3233 (mbr)		
ν_s C=O $_{(OAc)}$			1679 (wsh)				1743 (w)
			1645 (wsh)	1679 (wsh)		1679 (w)	
ν_s C=O $_{(NQox)}$	1629 (s)	1655 (m)		1645 (w)			
ν_s C=O $_{(NQox)}$						1641 (w)	
ν_s C=N	1579 (s)	1583 (s)		1606 (s)			
ν_s C=O $_{(p\text{-}NSQox)}$			1585 (s)		1580 (s)	1579 (s)	1579 (s)
ν_s C=N+ν_sC=C			1529 (s)		1534 (s)	1517 (s)	1548 (s)
ν_s C–O $_{(at\ C\text{-}2)}$	1211 (s)	1205 (s)	1228 (s)	1240 (s)	1238 (s)	1234 (sbr)	1228 (s)
ν_s N–O	1051 (s)	1045 (s)	1029 (w)	1087 (s)	1033 (w)	1031 (w)	1022 (w)
ν_s M–O–M				615 (s)			623 (s)

mbr – medium broad; s – strong; w – weak; sbr – strong broad; wsh – weak shoulder

centage mass loss and energy of activation at different steps in the pyrolytic reactions for **M-1**, **M-2**, **M-3A**, **M-3B** and **M-4** are presented in Table 3.

The kinetic parameters were calculated from the dynamic TG curves using the computer programs developed in our department with the help of rising temperature expression of Coats and Redfern [19]. Activation energies (E_a) were quantitized from kinetic plots obtained at two different heating rates, with best fit correlation coefficient r=0.999. The E_a values for two rates are within an accuracy range of ±3 kJ mol^{-1}. Table 3 represents best fit kinetic parameters for one heating rate only. The enthalpies for the different groups lost in **M-1**, **M-2** and **M-4** compounds are depicted in Table 4. The energies required for expulsion of L-1 in dimer, trimer and tetramer compounds of L-1 viz. **M-1**, **M-3A** and **M-4** turns out to be 29.8, 23.6 and 23.6 kJ mol^{-1} respectively. Hence average activation energy for expulsion of L-1 in these manganese clusters is calculated to be ~25.66 kJ mol^{-1}. Similarly in **M-3B** trimer of L-2 this energy is found to be ~20.42 kJ mol^{-1}. Our former report [20] on dehydration of quinone oxime chelates suggests that the energy required for release of ligand from its coordination in $NSQ^{\cdot}_{ox}$ form is ~23 kJ mol^{-1}. This infers presence of radical coordination of quinone cofactor in **M-1**, **M-3A**, **M-3B** and **M-4** clusters. In pyrolytic reaction of **M-2**, the E_a for the expulsion of L-2 is found to be ~ 42.15 kJ mol^{-1} (*cf.* Step III in Table 3) which is in accordance with the stabilization energy for the keto- form of L-2 (~ 41.08 kJ mol^{-1}) calculated using B3LYP method [8]. Hence, we can conclude that L-2 is coordinated in its fully oxidized NQ_{ox} form in **M-2**. Using additive property of activation energies the energy required for release of oxygen from third step of **M-2** is calculated to be 17.03 kJ/atom [118.36–2×42.15(L-2)=34.06(2 O)].

Energetics of coligand and counter ions

If water as substrate should bind to WOC cluster of 'S–state' cycle in PS-II, it needs energy of ~28 kJ mol^{-1}[14]. In proposed mechanism of water oxidation, it binds to the terminal Mn site where there is a competition of water entity to enter the coordination sphere with coligands such as O⌒O donor 'acetate' (OAc), O⌒N donor 'amino acids'. If the binding energies are comparable with auxillary ligands in coordination sphere then water can enter the coordination sphere of terminal Mn-site. Therefore, logically in model compound, the auxiliary ligands must have comparable energies ~28 kJ mol^{-1}. If trimers and tetramers are candidates of WOC models, then acetate and tyrosyl radical (amino acid)-type auxillary ligands are most significant at active site. Our O⌒N donor-type L-1, with E_a ~23.60 kJ mol^{-1} in **M-3A** trimer corresponds to radical $NSQ^{\cdot}_{ox}$ form which may compete with water. So also the acetate functional group evolved in step-II of **M-3A** also possesses comparable energy i.e. 27.09 kJ mol^{-1} with water. Here possible reductive elimination of acetates (step-II 180–255ºC) may be thought of at 200ºC similar to mixed carboxylates of manganese [21]. Using additive property of E_a in **M-4** tetramer we can estimate E_a

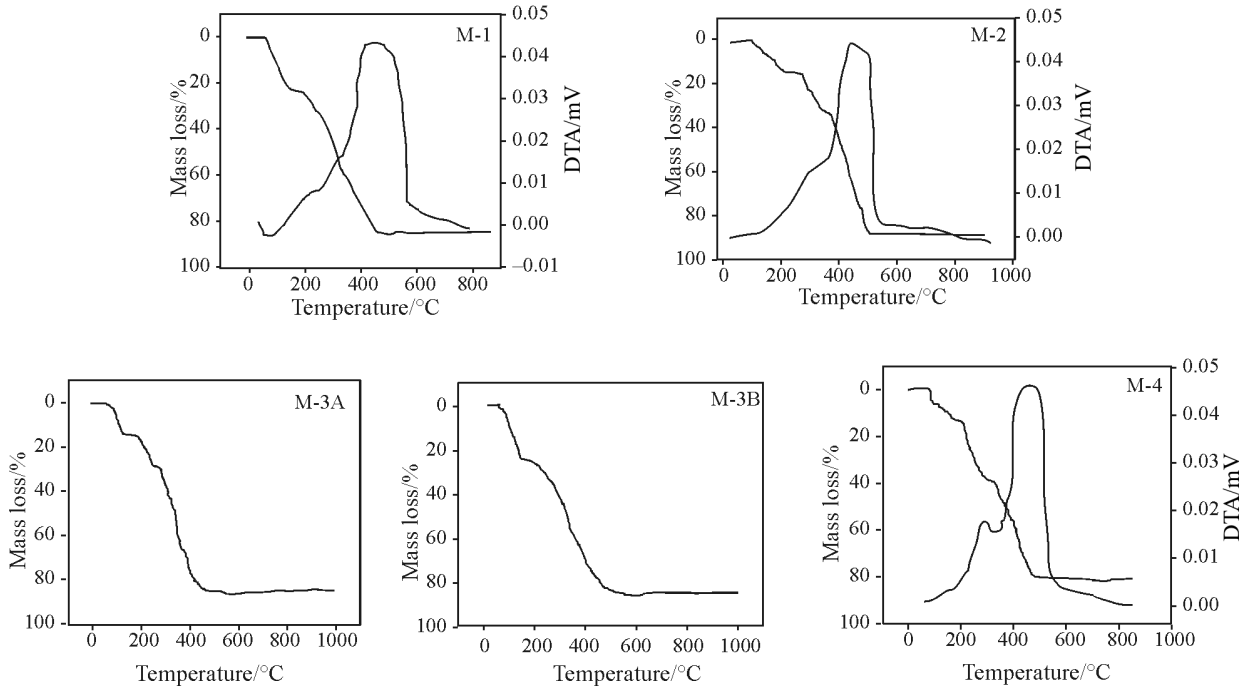

Fig. 1 TG plots of **M-1**, **M-2**, **M-3A**, **M-3B** and **M-4** together with DTA plots of **M-1**, **M-2** and **M-4**

Table 3 Data on activation energies (kJ.mol^{-1}) from TG in air for **M-1**, **M-2**, **M-3A**, **M-3B** and **M-4** compounds

Compound	Step no.	Temp. range/ °C	Mass loss (calc)/%	Probable composition of group lost	Residues	Order/ *n*	E_a/kJ	E_a/ kJ mol^{-1}
M-1	I	60–180	26.50 (26.70)	3OAc	Mn_2(L-1)$_2$	1.85	35.79	11.93
	II	210–475	57.50 (56.73)	2L-1	2MnO	1.95	59.61	29.80
M-2	I	75–250	16.67 (16.39)	$(C_2H_5)_4N$	$Mn_2O_2(OAc)_2$(L-2)$_2$	1.25	38.47	38.47
	II	265–340	14.00 (14.86)	2OAc	Mn_2O_2(L-2)$_2$	1.3	161.46	80.73
	III	340–550	56.66 (54.92)	2O+2L-2	Mn_2O_3	1.8	118.36	17.03/(O) 42.15/(L-2)[b]
M-3A	I	60–160	14.50 (16.35)	3OAc	$Mn_3(OAc)_3$(L-1)$_3$	1.49	27.87	9.29/(OAc)[c]
	II	180–255	14.00 (16.35)	3OAc	Mn_3(L-1)$_3$	0.4	81.28	27.09/(OAc)[c]
	III	265–475	57.50 (52.12)	3L-1	Mn_3O_4	1.9	70.81	23.60
M-3B	I	70–175	26.00 (26.24)	5OAc	Mn_3(OAc)(L-2)$_3$	1.9	45.31	9.06/(OAc)[c]
	II	200–500	59.00 (59.16)	OAc+3L-2	Mn_3O_4	2.8	70.57	9.29/(OAc)[c] 20.42/(L-2)[b]
M-4	I	70–175	13.50 (11.71)	$(C_2H_5)_4N$	$Mn_4O_2(OAc)_6$(L-1)$_2$	1.35	37.82	37.82
	II	200–300	27.00 (26.53)	5OAc	Mn_4O_2(OAc)(L-1)$_2$	1.59	68.25	13.65/OAc)[c]
	III	325–500	40.15 (42.00)	OAc+2O+ 2 L-1	2 Mn_2O_3	1.05	105.90	23.60/(L-1)[a] 17.03/(O) 24.64/(OAc)[c]

[a]L-1, Lawsone oxime, [b]L-2, Phthiocol oxime [c]OAc, acetate group

of one mole of OAc evolved in step-III as ~24.64 kJ mol^{-1} , substituting L-1 value from clean step of **M-3A** as 23.60 kJ mol^{-1} [105.9–2·17.03(2O)–2·23.60(2L-1)=24.64 kJ/(OAc)] . In pyrolytic reactions of **M-4** tetramer and **M-3A** trimer, two types of OAc ligands are involved. Type 1 having E_a comparable to L-1 as discussed above which are taking part in redox reaction while, type 2 having lower E_a (viz. 9.29 kJ/OAc in **M-3A** step-I and 13.65 kJ/OAc in **M-4** step-II) which may be simply acting as aggregator or bridging ligands, as shown in their structures I and II for **M-3A** and **M-4** respectively.

M-3B trimer also exhibits type 2 kind of bridging for OAc ligands which are expelled in Ist step with E_a of ~ 9.06 kJ mol^{-1}. Although **M-3A** and **M-3B** are

Table 4 Data from DTA in air for **M-1**, **M-2** and **M-4** compounds

Compound	Peak	Step	Group lost	Temp. range/ºC	ΔH/kJ g^{-1}	ΔH/kJ mol^{-1}
M-1	Endothermic	I	3(OAc)[c]	20–140	0.050	3.00
	Exothermic	II	2(L-1)[a]	210–620	1.669	315.72
M-2	Exothermic	II	2(OAc)[c]	210–340	0.112	6.635
	Exothermic	III	2(O) + 2(L-2)[b]	340–540	2.755	0.591 552.2
M-4	Exothermic	II	5(OAc)[c]	210–330	0.146	8.620
	Exothermic	III	1(OAc)[c]	330–520	1.756	3.00
			+2(O) +			0.591
			2(L-1)[a]			315.72

[a]L-1=Lawsone oxime, [b]L-2=Phthiocol oxime, [c]OAc=acetate.

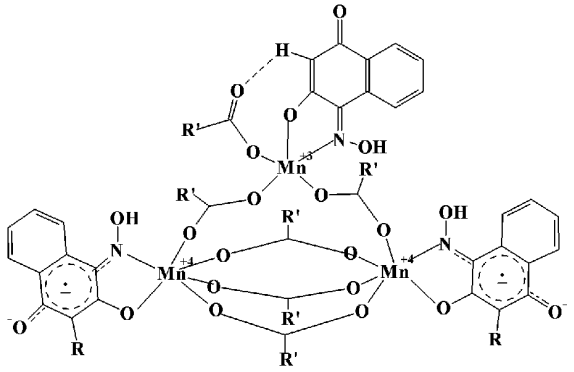

Structure I: **M-3A** where, *R*=H and *R′*=CH_3

synthesized using similar synthetic routes, former decomposes in three steps while latter shows two steps decomposition. The reductive elimination of OAc is observed in II[nd] step of **M-3A** which may result into reduction of apical Mn from +3→+2 oxidation state or *p*-NQ_{ox} → *p*-$NSQ^{\cdot-}_{ox}$ form, however in **M-3B**, out of six acetates, five evolves in step-I while one OAc eliminates with L-2 ligand in step- II. The latter OAc may be participating in the reduction of NQ_{ox} form to $NSQ^{\cdot-}_{ox}$ form during it's expulsion instead of further reduction of apical Mn^{2+} as shown in corresponding structures (I and III).

The energetics of M-4 from pyrolytic reactions indicate that terminal L-1 coordinates in one electron reduced $NSQ^{\cdot-}_{ox}$ form. Although synthetic routes followed for synthesizing **M-2** (using L-2) and **M-4** (using L-1) are similar, however, **M-2** results into dimer and **M-4** as tetramer. This may partly be attributed to steric hindrance engendered by the bulky methyl groups at C-3 position of L-2 which restricts **M-2** in dimer form and absence of such hindrances in L-1 facilitating formation of tetramer in **M-4**. Further, the counter ion $[(C_2H_5)_4N]^+$ used to stabilize these compounds is released in the first step of decomposition with a comparable E_a~38.47 kJ mol^{-1} and ~37.82 kJ mol^{-1} in **M-2** and **M-4**, respectively. Hence, the charge balance in their coordination sphere must also be similar. Thus the energies resulting in charge balance due to electron transfer for L-2 in **M-2** dimer (~42.15 kJ mol^{-1}) is almost equal to the energies of OAc and L-1 in **M-4** tetramer

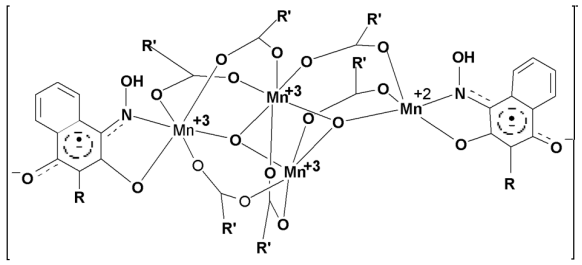

Structure II: M-4 where, *R*=H and *R′*=CH_3

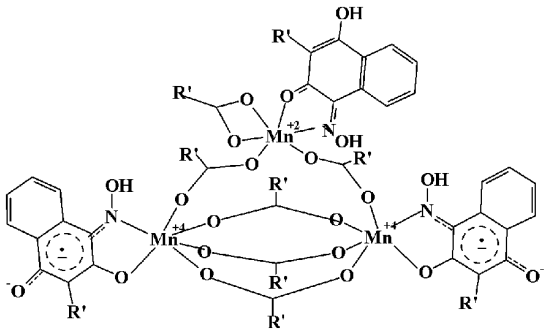

Structure III: M-3B where, *R′*=CH_3

(48.24 kJ mol^{-1}). The coordination of L-1 in **M-4** as radical $NSQ^{\cdot-}_{ox}$ form is attributed to the presence of bridged OAc function which acts as electron donor [22] in order to reduce L-1 ligand and stabilize **M-4**, while L-2 exhibits coordination within **M-2** in NQ_{ox} form where terminal OAc coligands are not at all involved in electron transfer with L-2 ligand and therefore evolved in second step with quite high energy (~80 kJ mol^{-1}). And this type of OAc may perform third category of terminal ligands as shown in structure (IV).

The stoichiometries for pyrolytic reaction of **M-1**, **M-2** and **M-4** at different steps in DTA are displayed in Table 4. DTA shows oxidative pyrolysis of L-1 and L-2 as exothermic peaks (cf. Fig. 1). Heat of reaction per step is calculated by considering simple Gaussian curve [23, 24]. An exotherm is observed for the decomposition of OAc auxillary ligand in **M-2** and **M-4** at high temperature range ~210–340°C. This is in contrast with the expulsion of OAc in **M-1** resulting from sublimation of acetic acid [25] at 110°C which is an endothermic reaction [17] where OAc may be abstracting hydrogen atom from reduced ligated 4-$HNSQ^{\cdot-}_{ox}$ forms [26]. The ΔH of OAc is found to be 3.00 kJ mol^{-1}. The heat of reaction for the evolution of L-1 in **M-1** turns out to be ~315.72 kJ mol^{-1} which is assigned to the reduced $NSQ^{\cdot-}_{ox}$ form of L-1

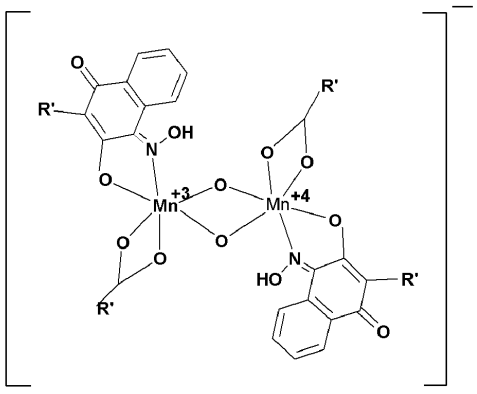

Structure IV: M-2 where, *R′*=CH_3

as concluded in TG studies. Since L-1 is present in NSQ^{-}_{ox} form in **M-4** as well, using additive property of enthalpy, we can estimate ΔH of oxygen in **M-4** as 0.591 kJ atom^{-1} [1.756–1.669–0.050=0.037 kJ g^{-1}. (0.037×15.999/1000)=0.591 kJ/O atom]. **M-2** exhibits an exotherm at a temperature range 340–540°C for the expulsion of oxygen and L-2. By substituting ΔH of oxygen (as calculated from **M-4**) in **M-2** the heat of reaction for L-2 can be quantized as 552.29 kJ mol^{-1}. Thus, existence of redox forms of L-1 and L-2 viz. NQ_{ox} in **M-2** and NSQ^{-}_{ox} in **M-1** and **M-4** are confirmed as also depicted in their TG results.

Powder X-ray diffraction studies

The synthetic route adapted for **M-2** and **M-4** were similar, however **M-2** results into dimer and **M-4** forms tetramer (also observed in supra thermal data) hence, it is interesting to analyze their residues. The PXRD pattern for the residues of **M-2** and **M-4** complexes obtained after thermal decomposition in 2θ range of 20–80° is displayed in Fig. 2. The diffraction pattern recorded for **M-2** matches reasonably well with the lines of hexagonal Mn_2O_3 structure [27] reported with following lattice parameters a=b=5.00 Å and c=15.00 Å. A strong (110) line at 2θ=36.3° together with medium intensity lines (104, 116, 124 and 030) at 2θ=32, 52.6, 61.5 and 63.2° respectively indicate better crystallinity of Mn_2O_3 in **M-2** as compared to crystallinity of Mn_2O_3 in **M-4** (a=b=5.39 Å and c=13.96 Å). The residue of latter also demonstrates presence of cubic face centered MnO [28] with lattice parameters as a=b=c=4.439 Å in addition to hexagonal Mn_2O_3. PXRD of **M-4** shows a strong (110) line at 2θ=35.2°characteristic of Mn_2O_3 together with a line (111) at 2θ=35.8° corresponding to d=2.568 Å in MnO. An additional line at 2θ=59.5° is characteristic of (220) plane of cubic (FC) MnO which is absent in **M-2**. Due to mixture of oxides viz. Mn_2O_3 and MnO in **M-4** residue, the signals are broader in PXRD of **M-4** as compared to that of **M-2**. The differences in resultant residues of **M-2** dimer and **M-4** tetramer may be caused due to different types of coordination of spin – carrier L-2 and L-1 ligands as seen in TG-DTA studies.

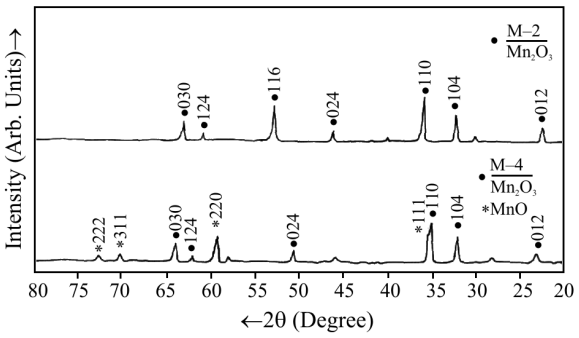

Fig. 2 Powder X-ray diffraction patterns of **M-2** and **M-4** compounds

Finally, we can conclude that the energetics quantitized from thermal studies, suggest the relevant roles of various functional groups in WOC model compounds. Our contribution towards functional model in PS-II for manganese dimer of L-1 is reported earlier [3, 29], however, recent reports on crystal structure of oxygen evolving complex in PS-II from *Thermosynechococcus vulcanus* and *Thermosynechococcus elongates* bacteria [5] projects tetrameric manganese cluster through 3+1 organization. With this view **M-3A**, **M-3B** and **M-4** may be extremely significant. Therefore, in future, our trimers and tetramer with effective spin transfer mimicking S_2Y_Z type interactions may also act as good candidates for WOC in PS-II [30].

Acknowledgements

AVT is thankful to Bhabha Atomic Research Centre (BARC) for providing research fellowship through collaborative scheme of Pune University-BARC, Mumbai, India.

References

1 K. Prassides, Mixed Valency Systems: Applications in Chemistry, Physics and Biology, U.k, Kluwer Academic Publishers (1991).
2 S. A. Richert, P. K. S. Tsang and D. T. Sawyer, Inorg. Chem., 27 (1988) 1814.
3 S. I. Allakhverdiev, M. S. Karacan, G. Somer, N. Karacan, E. M. Khan, S. Y. Rane, S. B. Padhye, V. V. Klimov and G. Renger, Biochemistry, 33 (1994) 12210.
4 J. J. Low and W. A. Goddard, III. J. Am. Chem. Soc., 108 (1986) 6115.
5 a. A. Zouni, H.-T. Witt, J. Kern,, P. Fromme, N. Krauss, W. Saenger and P. Orth, Nature 409 (2001) 739.
b. Nobuo Kamiya and Jian – Ren Shen, Proc. Natl. Acad. Sci. U.S.A., 100 (2003) 98.
6 C. G. Pierpont, Coord. Chem. Rev., 216 (2001) 99.
7 C. G. Pierpont, Coord. Chem. Rev., 219 (2001) 451.
8 D. R. Thube, A. V. Todkary, K. Joshi, S. Y. Rane, S. A. Salunke, F. Varret, J. Marrot and S. P. Gejji, J. Mol. Struct. (THEOCHEM) 622 (2003) 211.
9 D. D. Perrin, W. L. F Armargo and D. R. Perrin, Purification of Laboratory Chemicals, Pergamon, London, 1966.
10 S. Y. Rane, S. B. Padhye, E. M. Khan and P. L. Garge, Synth. React. Inorg. Met- Org. Chem., 18 (1988) 609.
11 J. B. Vincent, K. Folting, J. C. Huffman and G. Christou, Inorg. Chem., 25 (1986) 996.
12 S. Y. Rane, S. B. Padhye, G. N. Natu, A. H. Kumar and E. M. Khan, J. Thermal Anal., 35 (1989) 2331.
13 S. S. Gawali, R. Dalvi, Ah. Khursheed and S. Rane, J. Therm. Anal. Cal., 76 (2004) 804.
14 C. Tommos and G. T. Babcock, Acc. Chem. Res., 31 (1998) 18.

15 D. H. Williams and M. S. Westwell, Chem. Soc. Rev., 27 (1998) 163.
16 J. Berstein, M. C. Etter and L. Leisserowitz, The role of Hydrogen bonding in Molecular Assemblies in Structure Correlation Ed; H. B. Bürgi and J. D. Dunitz, VCH, Weinheim, (1994) 431.
17 S. Y. Rane, J. P. Salvekar, N. V. R. Dass, P. S. Kaduskar and P. P. Bakare, Thermochim. Acta, 191 (1991) 255.
18 H. Visse, C. E. Dube, W. H. Armstrong, K. Sauer and Vittal K. Yachandra. J. Am. Chem. Soc., 124 (2002) 11008.
19 A. W. Coats and J. P. Redfern, Nature, 201 (1964) 68.
20 S. Y. Rane, S. B. Padhye, G. N. Natu, A. H. Kumar and E. M. Khan, J. Thermal Anal., 35 (1989) 2331.
21 H. Langbein, S. Christen and G. Bonsdorf, Thermochim. Acta 327 (1999) 173.
22 E. Bernard, S. Chardon –Noblat, A. Deronzier and J. M. Latour, Inorg. Chem., 38 (1999) 190.
23 W. W. Wendlant, Thermal Methods of Analysis, 2nd Edn. Wiley Interscience Publication N.Y. (1974) 184.
24 A. Blazek, Thermal Analysis, Van – Nostrand, Reinhold (1973)170.
25 N. A. Lange, Handbook of Chemistry, McGraw-Hill, New York, 1961.
26 M. M. Whittaker, D. P. Ballou and J. W. Whittaker, Biochemistry, 37 (1998) 8426.
27 JCPDS, card no. 33–900, Intenational centre for diffraction data, USA, 1984.
28 JCPDS, card no. 7–230, Intenational centre for diffraction data, USA, 1984.
29 S. I. Allakhverdiev, M. S. Karacan, G. Somer, N. Karacan, E. M. Khan, S. Y. Rane, S. B.. Padhye, V. V. Klimov and G. Renger, Z. Naturforsch., 49c (1994) 587.
30 K. V. Lakshmi, S. S. Eaton, G. R. Eaton, H. A. Frank and G. W. Brudvig, J. Phys. Chem. B, 102 (1998) 8327.

Received: November 20, 2004
In revised form: February 15, 2005

DOI: 10.1007/s10973-005-6529-7